Photoinduced Charge Transfer between CdSe Quantum Dots and *p*-Phenylenediamine

Shailesh N. Sharma,† Zeena S. Pillai, and Prashant V. Kamat*

Notre Dame Radiation Laboratory, Notre Dame, Indiana 46556-0579

Received: January 15, 2003; In Final Form: July 8, 2003

The excited state interaction between CdSe nanocrystals and a hole acceptor, *p*-phenylenediamine (PPD), is probed using emission and transient absorption spectroscopies. The changes in the photophysical properties of CdSe nanocrystals arising from the interaction with PPD are compared with an aliphatic amine, *n*-butylamine (*n*-BA). At low concentrations (<0.5 mM) *n*-butylamine enhances the emission of CdSe quantum dots whereas PPD effectively quenches the emission at similar concentrations. The low oxidation potential of PPD (E° = 0.26 V vs NHE) enables it to act as an effective scavenger for photogenerated holes. A surface bound complexation equilibrium model has been proposed to explain the quenching phenomenon. The transient absorption measurements confirm the formation of PPD cation radical and subsequent formation of coupling product. Formation of such charged species at the surface extends the bleaching recovery over several microseconds.

Introduction

Size-controlled semiconductor nanocrystallites with a narrow size distribution have drawn the attention of scientists and engineers of various disciplines. CdSe quantum dots have been shown to be advantageous in biological labeling experiments and as chromophores in light-emitting diodes.[1−3] Their importance in nanoelectronics, light energy conversion, and biological applications have made them ideal candidates for studies involving semiconductor quantum dots. Steigerwald et al.[4,5] synthesized nanometer-size CdSe clusters using organometallic reagents in inverse micellar solution followed by chemical modification of the surface of these clusters. In later years the TOPO (trioctylphosphine oxide) capping method[6,7] was developed to synthesize size-controlled CdSe nanocrystals of highest monodispersity (standard deviation less than 5%). Capping of CdSe colloids formed at high temperature (573 K) with TOPO facilitated stabilization against particle growth.

One of the interesting photophysical properties of the CdSe nanocrystals is the blinking emission behavior. The on−off emission cycles of a single nanocrystal under an extended period of photoillumination have been monitored by several researchers using optical microscopy.[8−16] Under band gap excitation, metal chalcogenide nanoparticles are known to photoionize and become positively charged.[17,18] Dependence of the photoionization rate on the electron surface confinement barrier has been investigated using electrostatic force measurements (EFM). CdSe nanocrystals modified with different surface passivating molecules were employed for these measurements.[9,19] Furthermore, electric field studies have revealed the presence of local electric fields that are thought to result from photoionization and/or trapped charges on or near the surface of the nanocrystallite. The changes in surface charging over time further induce spectral diffusion on the time scale of a typical single-nanocrystallite emission spectrum.[20] The effect of excess positive holes on chalcogenide emission has been probed using radiolytically generated radicals.[21] A 5-fold increase in the observed fluorescence intensity of CdSe nanocrystal and a striking reduction in their fluorescence blinking behavior has been achieved via electromagnetic interactions with a rough metal film.[12] Introduction of surface hole traps were found to enhance and prolong the IR absorption in photoexcited quantum dots.[22] Thus, the molecular interactions at the CdSe surface play an important role in controlling the excited state dynamics.

The interaction between single crystal CdSe and amines has been the topic of many earlier investigations (see ref 23 for a detailed review). Direct interaction between the CdSe surface and amine functional group passivates the surface and blocks the trapping of electrons at the defect sites. This observation has been well documented for CdS and CdSe semiconductor nanoparticles.[24−28] On the other hand, for TOPO-capped CdSe nanocrystals El-Sayed and co-workers report a decreased emission yield at high concentrations of butylamine with no specific change in the emission decay lifetime.[29] These researchers attributed the quenching behavior to the electron-donating property of *n*-butylamine. Since the oxidation potential of amines vary over a wide range, their interaction with CdSe can produce different results. To further assess the role of surface-bound species, we have selected an aromatic amine with relatively low oxidation potential so that we can directly probe the interfacial charge transfer at the CdSe nanocrystals. We have chosen *p*-phenylenediamine as a hole acceptor since its oxidation potential is lower than the valence band edge of CdSe. The emission and transient absorption measurements that illustrate the differing interaction of two amines (viz., *n*-butylamine and *p*-phenylenediamine) with CdSe nanocrystals are presented.

Experimental Section

Materials and Methods. The materials used were of the purest quality available and used as received. Absorption spectra were recorded using a Shimadzu 3100PC Spectrophotometer. Steady state emission spectra were recorded using an SLM-Aminco 8100 spectrofluorometer. Emission lifetime measurements were performed using a laser strobe fluorescence lifetime spectrometer (Photon Technique International). The excitation was carried out using a 337 nm pulsed N_2 laser.

Synthesis of CdSe Nanoparticles. CdSe nanocrystals were prepared using the method described by Peng et al.[30] CdO

* Address correspondence to this author. E-mail: pkamat@nd.edu.
† On leave from National Physical Laboratory, New Delhi 110012, India.

10.1021/jp034109f CCC: $25.00
Published on Web 08/22/2003

(0.0514 g), tetradecylphosphonic acid (TDPA, 0.2232 g), and trioctylphosphine oxide (TOPO, 3.7768 g) were loaded into a 250 mL flask. The mixture was then heated to ~320 °C under Ar flow and stirring. Once the CdO was dissolved in the TDPA and TOPO mixture, the temperature of the solution was cooled to 270 °C. A solution of Se powder (0.0411 g) dissolved in 2.4 mL of trioctylphosphine (TOP) was quickly injected into the flask. After the injection, the CdSe nanocrystals were allowed to age at 250 °C for 5 min before cooling to room temperature under argon atmosphere. This preparation typically yields ~4 nm diameter CdSe nanocrystals. By increasing the molar ratio of Cd:Se from 1:1 to 2:1, we were able to produce 3 nm diameter CdSe nanocrystals. These nanocrystals were suspended in toluene and purged with nitrogen for absorption and emission measurements. The absorbance of the suspension was adjusted to 0.3 at the excitation wavelength.

Nanosecond Laser Flash Photolysis. Time-resolved absorption experiments were performed using a Spectra Physics Nd:YAG laser system (532 nm, output 10−20 mJ/pulse, pulse width ~10 ns). A typical experiment consisted of a series of three to five replicate shots at a single monitoring wavelength. The signals from the photomultiplier were processed by a 7200 LeCroy digital storage oscilloscope. The whole experiment was controlled by a desktop computer. Cutoff filters were used to avoid spurious responses from second-order scattering from the monochromator gratings. The details of the experimental setup can be found elsewhere.[31]

Results and Discussion

Absorbance and Emission Characteristics. Size quantization effects markedly influence electronic and optical properties of semiconductor materials.[32−34] In a chemical precipitation method, a variety of approaches have been considered to arrest the growth of particles of desired size. For example, control of the water pool size in a reverse micellar system yields size-quantized CdS and CdSe particles of 3−5 nm diameter.[28,35] Since reverse micelles form a dynamic system, whereby water pools continuously exchange their contents though intermicellar collisions, we observe a slow growth in particle size. Attempts have been made earlier to cap these colloids with organic ligands or large band gap semiconductors[4,36] and control the growth of semiconductor nanoparticles. TOPO-capped CdSe colloids on the other hand provide good protection against particle growth. This method is also convenient for binding a variety of organic molecules strongly to the CdSe surface by exchanging with the TOPO layer. Bulk CdSe, which exists in both wurtzite and zinc blende forms, exhibits a bulk band gap at 1.83 eV (689 nm).[37] Nanocrystals of CdSe prepared at high temperatures exhibit the wurtzite structure,[7] while thiol-capped CdSe clusters prepared at low temperature exhibit zinc blende structure. [38] Bulk CdSe was prepared by the reaction of $CdSO_4$ and Na_2SeSO_3 in aqueous medium. Based on the absorption onset, we expect the band gaps of these two CdSe nanoparticles to be 2.08 and 2.3 eV, respectively. The fact that the emission maximum lies close to its absorption onset indicates the emission arises from direct recombination between conduction and valence band charge carriers.

The emission yield of these quantum dots was measured using Rhodamine 6G as reference ($\Phi_f = 0.96$ in ethanol). The emission yields for 3 and 4 nm CdSe quantum dots were 0.18 and 0.016, respectively. These widely different emission yields indicate that the ratio of Cd:Se can significantly influence the radiative charge recombination process. Higher Cd^{2+} concentration employed in the preparation of 3 nm CdSe nanoparticles has a beneficial effect in enhancing the radiative charge recombination process. These observations parallel earlier preparations of metal chalcogenide nanoparticles in which excess Cd^{2+} was employed to enhance the emission yield.[39,40] Termination of the surface with Cd^{2+} instead of Se^{2-} passivates the surface traps that facilitate nonradiative charge recombination. Termination of the nanocrystal surface with ZnS or ZnSe also yields a similar enhancement in the emission yield.[41,42]

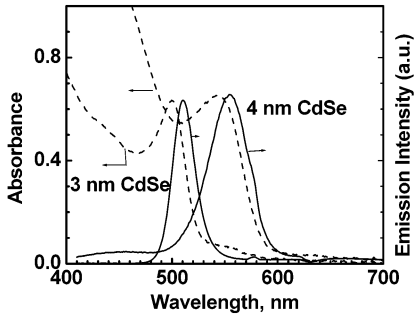

Figure 1. Absorption (---) and emission (—) spectra of (A) 3 and (B) 4 nm diameter, TOPO-capped CdSe nanocrystals suspended in toluene.

Influence of n-Butylamine and p-Phenylenediamine on the Emission Yield of CdSe Quantum Dots. Parts A and B, respectively, of Figure 2 show the emission spectra of 4 nm CdSe nanoparticles in the presence of varying amounts of *n*-BA and PPD. Two distinctively different trends were evident as we increase the concentration of amine from 0 to 1.0 mM for *n*-BA and 0−0.5 mM for PPD, respectively. With increasing concentration of *n*-BA we see an enhancement in the emission yield, and at concentrations around 1.0 mM emission yield saturates. At these concentration levels most of the CdSe particle surface is complexed with *n*-BA. The fact that the emission maximum and spectral shape are independent of amine concentration rules out formation of new surface states. The complexation of *n*-BA passivates the surface and suppresses nonradiative recombination at surface vacancies. Such surface complexation methods are useful to enhance the luminescence yields of low emitting semiconductor quantum dots. These observations parallel the enhancement observed with surface modification of CdSe using a variety of different amines.[23,27] However, the CdSe emission quenching observed at relatively high concentration of *n*-BA is in contrast to the present observation.[29,43] It is likely that the high concentration of *n*-BA employed in these studies introduces an additional pathway for the nonradiative recombination processes.

In the case of PPD, we see a quenching of the emission. Nearly all the emission from CdSe quantum dots is quenched at the concentration level of 0.5 mM. The fact that PPD is an effective quencher (even at low concentrations) for CdSe emission suggests that it is capable of directly intercepting one of the charge carriers, thus disrupting the radiative recombination process (reactions 1 and 2).

$$\mathrm{CdSe} + h\nu \rightarrow \mathrm{CdSe(h + e)} \rightarrow \mathrm{CdSe} + h\nu' \qquad (1)$$

$$\mathrm{CdSe(h)} + \mathrm{PPD} \rightarrow \mathrm{CdSe} + \mathrm{PPD}^{+} \qquad (2)$$

Since the oxidation potential of PPD is 0.26 V vs NHE, it can effectively scavenge the photogenerated holes from the CdSe surface. Note that valence band edge of CdSe quantum dot is expected to be around +1.2 V vs NHE. Both the size quantization effect and surface-bound ligands are expected to shift the valence band to more positive potentials, thus making it a stronger oxidant than the bulk.[44,45] However, this shift in valence band is likely to be ≤0.5 V and is not sufficient to

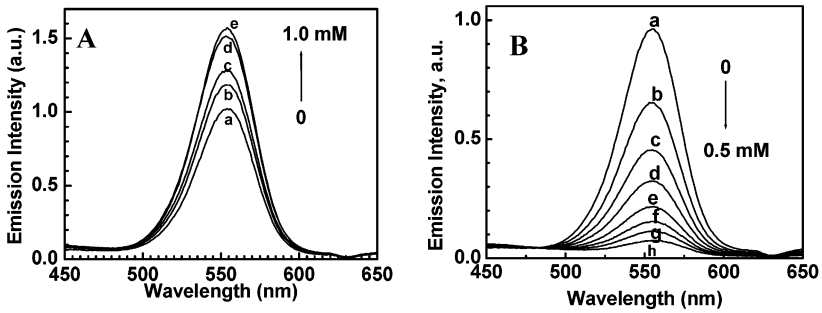

Figure 2. Effect of (A) *n*-BA and (B) PPD on the emission of CdSe nanoparticles (4 nm diameter). The concentrations of *n*-BA were (a) 0, (b) 0.05, (c) 0.175, (d) 0.5, and (e) 1.0 mM. The concentrations of PPD were (a) 0, (b) 0.01, (c) 0.025, (d) 0.05, (e) 0.1, (f) 0.175, (g) 0.275, and (h) 0.5 mM. (Emission spectra were recorded using 380 nm excitation.)

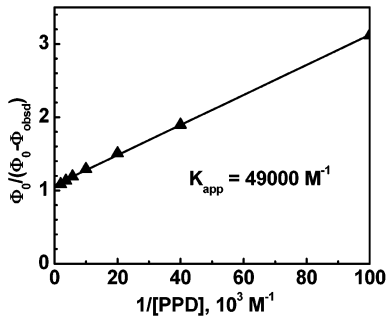

Figure 3. Plot of $\Phi_0/(\Phi_0 - \Phi_{obsd})$ versus reciprocal concentrations of PPD.

oxidize *n*-BA. (The oxidation potential of *n*-BA is >1.9 V versus NHE.) Thus we observe effective scavenging of photogenerated holes only by PPD. One can employ a size-dependent molar extinction coefficient of CdSe particles to determine the average number of molecules bound to each CdSe particle.[6,46] We have employed a simple complexation model to determine the association of amines with CdSe by considering association equilibrium 3:[47]

$$\text{CdSe} + \text{PPD} \leftrightarrow \{\text{CdSe}\cdots\text{PPD}\} \qquad (3)$$

K_{app} is the apparent association constant. We can then express the observed emission yield (ϕ_{obsd}) in terms of uncomplexed (ϕ^0_{em}) and complexed (ϕ'_{em}) CdSe quantum dots with PPD.

$$\phi_{obsd} = (1 - \alpha)\phi^0_{em} + \alpha\phi'_{em} \qquad (4)$$

where α is the degree of association between CdSe and PPD and can be equated to the term K_{app}[PPD]/[1 + K_{app}[PPD]. Equation 3 can be further simplified to the expression

$$\phi^0_{em}/(\phi^0_{em} - \phi_{obsd}) = \phi^0_{em}/(\phi^0_{em} - \phi'_{em}) + \phi^0_{em}/\{K_{app}(\phi^0_{em} - \phi'_{em})[\text{PPD}]\} \qquad (5)$$

Based on this analysis, we expect a linear relationship between $\phi^0_{em}/(\phi^0_{em} - \phi_{obsd})$ and 1/[PPD]. Indeed, the linear plot in Figure 3 supports our argument that the interaction between CdSe and PPD involves complexation equilibrium. Based on the slope and the intercept of the linear plot in Figure 3, we obtain the value of K_{app} as 4.9×10^4 M^{-1}. Such a high value of K_{app} explains the strong affinity of CdSe surface to complex with PPD. We also would like to point out that earlier attempts to analyze the emission yield and decay on the basis of a Stern−Volmer plot produced a significant deviation from the normal linear behavior.[29] These researchers adopted a multiple binding site model to analyze the quenching of CdSe quantum dots by an aliphatic amine. By using a two-state selective binding model, they explained the steady state and dynamic type quenching behavior for CdSe−butylamine system. Although such a multiple binding site with a variable affinity is still possible in the present case, the high apparent association constant suggests that the magnitude of variations between the sites is quite minimal. The quenching results presented in Figures 2B and 3 show the validity of our analysis in adopting a model of association equilibrium for establishing the interaction between CdSe nanocrystals and PPD.

Emission Lifetimes. We further probed the interaction between CdSe and amines by monitoring the emission decay using 337 nm laser pulse as the excitation source. The emission intensity recorded at the emission maximum exhibited a multiexponential decay and was analyzed using biexponential decay kinetics (expression 6).

$$F(t) = a_1 \exp(-t/\tau_1) + a_2 \exp(-t/\tau_2) \qquad (6)$$

In the absence of any amine, the 3 nm CdSe nanoparticles exhibit lifetimes of 6.8 (40%) and 55.0 (60%) ns while 4 nm CdSe nanoparticles exhibit lifetimes of 6.8 (69%) and 33.25 (31%) ns, respectively. In the presence of *n*-BA the emission lifetimes did not exhibit any significant changes. A similar insensitivity of emission lifetime to the presence of *n*-BA has been reported for TOPO-capped CdSe quantum dots.[29,43] The origin of multiexponential emission decay of metal chalcogenides has been investigated in detail, and the explanation for such behavior varies from the distribution of trapping sites within the nanoparticle[48−50] to the blinking effects.[8,10,11] For single nanocrystal CdSe systems, the fluctuation in the decay lifetime of individual nanocrystals was regarded as the possible reason for observing multiexponential decay.[11]

To compare the emission lifetimes, we determined average lifetime value ($\langle t \rangle$) using expression 7.[51]

$$\langle t \rangle = \sum a_i \tau_i^2 / \sum a_i \tau_i \qquad (7)$$

By substituting the values of a_1, a_2, τ_1, and τ_2 in expression 7, we obtained the average lifetime values, and they are summarized in Figure 5 and Table 1. In the case of *n*-BA we observe little variation in the average lifetimes up to 0.5 mM. Although we observe an enhancement in the emission yield with increasing concentrations of *n*-BA, it has little effect on the emission decay behavior. Thus, the role of *n*-BA is to enhance the radiative charge recombination sites without affecting the decay kinetics radiative and nonradiative processes.

On the other hand, the decrease in the average lifetime observed with increasing PPD concentration parallels the decrease observed in emission yield. For 3 nm diameter CdSe particles we observe a decrease in average lifetime from 51.23

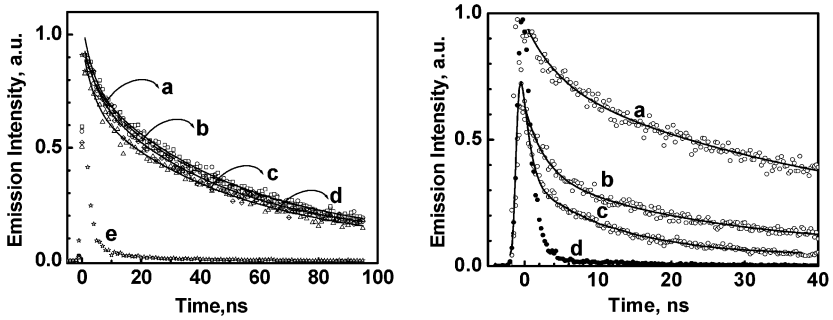

Figure 4. (A) Emission decay of 4 nm CdSe quantum dots in toluene containing different amounts of *n*-BA: (a) 0, (b) 0.05, (c) 0.175, and (d) 0.5 mM with scatter pulse shown in (e). (B) Emission decay of 4 nm CdSe quantum dots in toluene containing different amounts of PPD: (a) 0, (b) 0.1, and (c) 0.275 mM with scatter pulse shown in (d).

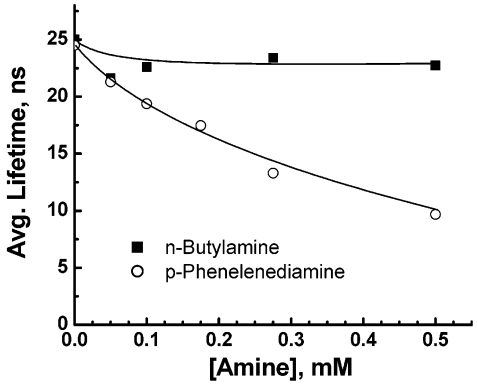

Figure 5. Comparison of average lifetimes of 4 nm CdSe quantum dots in the presence of *n*-BA and PPD. The average emission lifetimes were determined using expression 7.

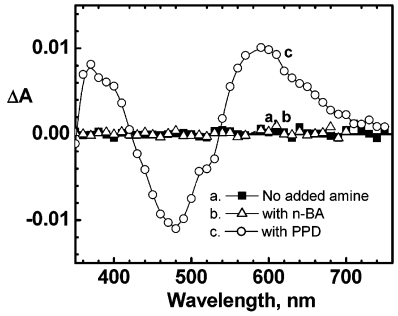

Figure 6. Transient absorption spectra recorded 20 μs after 532 nm laser pulse excitation of CdSe suspension in deaerated toluene: (a) no added amine; (b) in the presence of 1.0 mM *n*-BA; (c) in the presence of 2 mM PPD.

ns to 7.10 ns as we increase the PPD concentration from 0 to 0.5 mM. The observed decrease in the emission yield and lifetime is indicative of the fact that the PPD interaction with CdSe results in hole transfer quenching. If we assume that the scavenging of holes at the CdSe surface by PPD is the only process responsible for the observed decrease in emission lifetime, we can estimate the rate constant from expression 8.

$$k_{ht} = 1/\tau_{PPD} - 1/\tau \qquad (8)$$

where τ_{PPD} and τ are the CdSe emission lifetimes in the presence and absence of PPD. Upon substituting the values of lifetimes (at 0 and 0.5 mM PPD from Table 1) in expression 6, we obtain hole transfer rate constants of 1.23×10^8 and 0.63×10^8 s^{-1} for 3 and 4 nm CdSe particles, respectively. These rate constant values should be considered as an apparent value since they were determined from the average emission lifetime values.

Transient Absorption Studies. If indeed, the interaction of excited CdSe with PPD results in hole transfer, we should be able to monitor charge-transfer products using transient absorption spectroscopy. Nanosecond laser flash photolysis experiments were carried out using 532 nm laser pulse as the excitation source. The transient absorption spectra recorded 20 μs after laser pulse excitation are shown in Figure 6. CdSe quantum dots upon excitation with the laser pulse show no significant absorption changes in the 350−700 nm region. As discussed in earlier studies,[52,53] the majority of the photogenerated charge carriers undergo recombination without inducing any long-lived chemical transformations. The transient bleaching arising from charge separation, charge accumulation, and/or trapping of charge carriers is usually seen at subnanosecond time levels. These processes have been studied earlier by probing ultrafast processes with femtosecond and picosecond laser pulses.[47,53−58] The absence of long-lived bleaching or transient absorption in spectrum a (Figure 6) indicates the charge recombination processes are completed within the laser pulse duration and the CdSe nanocrystals remain stable during laser pulse duration.

CdSe nanocrystals in the presence of two amines, *n*-BA and PPD, exhibit two distinctively different spectral characteristics following 532 nm laser pulse excitation. The presence of *n*-BA did not produce any changes in the transient absorption recorded in the microsecond time scale. This further confirmed the argument made in an earlier section that the role of the aliphatic

TABLE 1: Photophysical Properties of CdSe Nanoparticles Suspended in Toluene at 295 K

CdSe diam, nm	amine (0.5 mM)	emission max, nm	emission quantum yield[a]	emission lifetimes,[b] ns τ_1 (%)	τ_2 (%)	av lifetime, ns
3.0		511	0.18	6.80 (40.1)	55.01 (59.9)	51.23
3.0	*n*-BA	511	0.21	4.06 (58.1)	50.92 (41.9)	46.25
3.0	PPD	512	0.012	0.10 (97.4)	9.70 (2.57)	7.10
4.0		555	0.016	6.79 (68.8)	33.25 (31.2)	25.04
4.0	*n*-BA	553	0.0227	6.21 (72.8)	31.47 (27.2)	22.74
4.0	PPD	560	0.00125	3.91 (92.6)	22.29 (7.4)	9.67

[a] Determined using Rhodamine 6G solution as reference. [b] The emission decay was analyzed using the expression $F(t) = a_1 \exp(-t/\tau_1) + a_2 \exp(-t/\tau_2)$, where τ_1 and τ_2 are the lifetimes. The values in parentheses indicate the fraction (%) of the corresponding lifetime component.

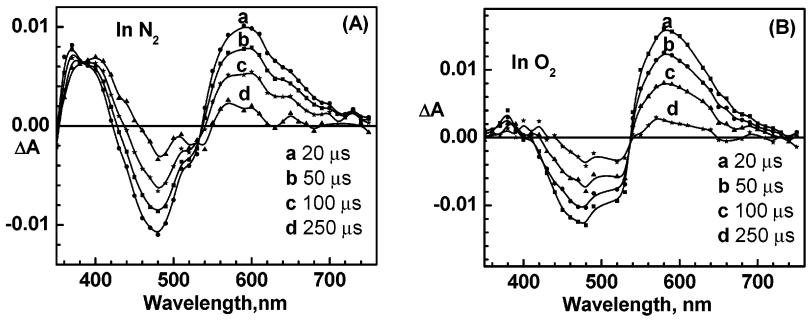

Figure 7. Time-resolved transient absorption spectra recorded after 532 nm laser pulse excitation of CdSe suspension in toluene containing 2 mM PPD. The spectra were recorded in (A) nitrogen-purged and (b) oxygen-purged suspensions at time intervals of (a) 10, (b) 50, (c) 100, and (d) 250 μs.

amine is merely to passivate the CdSe surface without directly intercepting photoinduced charge carriers. Surface binding of *n*-BA promotes the radiative recombination process as indicated by the increase in the emission yield. The presence of PPD, on the other hand, results in the formation of a long-lived transient with difference maxima at 370 and 600 nm. The bleaching in the 500 nm region indicates the depletion of CdSe absorption and hence its participation in the photoinduced formation of intermediates. The intermediate species formed following the excitation of CdSe quantum dots further show the ability of PPD to induce charge transfer interaction. A similar charge transfer interaction at semiconductor interface has been extensively studied in earlier work (see, for example, refs 59−62).

In Figure 7, we compare the time-resolved transient spectra recorded following 532 nm laser pulse excitation of N_2-purged and O_2-purged CdSe−PPD suspensions. As compared to N_2-saturated suspensions, the presence of O_2 has a marked effect on the transient absorption in the 360−420 nm region. This transient absorption is significantly suppressed in the presence of O_2. On the other hand, the transient absorption at 600 nm region remains unaffected. The insensitivity of the transient absorbing in the red region (viz., species with 600 nm absorption) to oxygen indicates that it is an oxidized product. The scavenging of holes by PPD is expected to produce $PPD^{\bullet+}$ cation (reaction 2). As shown earlier,[63] the PPD cation absorbs strongly in the 400−600 nm region with a maximum around 480 nm. Strong bleaching of CdSe in the 500 nm region overlaps with this spectrum and renders the difference absorption maximum to be shifted toward the red. Furthermore, the PPD cation radical is also known to undergo a coupling reaction with the parent amine to produce a dimer-like species with absorption in the red.[64]

The interfacial hole transfer to PPD is considered to be an ultrafast process. Burda et al.[52] estimate the hole transfer from CdSe nanocrystals to thiophenol to occur on the time scale of 3 ps. Once the photogenerated holes are scavenged by PPD, excess electrons accumulate within the CdSe nanoparticles. These electrons in turn interact with the Cd^{2+} to produce Cd^{+} and Cd^{0} sites (reaction 9).

$$(CdSe)_n(e)_m \rightarrow (Cd^{+}Se^{2-})_m(CdSe)_{n-m} \rightarrow (Cd^{0}Se^{2-})_{m/2}(CdSe)_{n-m/2} \quad (9)$$

The transient absorption at 380 nm essentially represents the changes associated with the electron localization at the CdSe surface. In the presence of O_2, these accumulated electrons are driven away, thereby regenerating the CdSe surface. If not neutralized with an electron donor or undergoing charge recombination, the process of electron accumulation can further lead to cathodic corrosion. More details on the absorption changes associated with electron/hole trapping and anodic and cathodic corrosion processes have been established earlier.[65,66]

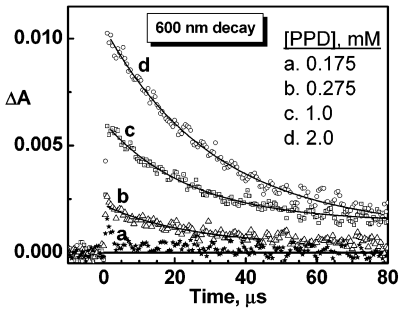

Figure 8. Absorption−time profile recorded at 600 nm following 532 nm laser pulse excitation of CdSe suspension in toluene containing (a) 0.175, (b) 0.275, (c) 1.0, and (d) 2.0 mM PPD.

The assignment of 600 nm absorption to the oxidized form of PPD was also confirmed by recording the absorption−time profiles at different hole acceptor concentrations (Figure 8). With increasing concentration of PPD we see an increase in the yield of oxidation product. This transient quickly decays with a lifetime of 30.0 ± 1.0 μs to yield a coupled product. The formation of such coupled products is often the basis of forming many colored dyes.[64] Another interesting observation in the spectra illustrated in Figure 8 is the fact that the majority of the transient bleaching recovers within the duration of ~100 μs. Only a small fraction (<5%) of the transient bleaching fails to recover, indicating the small probability of irreversible photochemical changes that occur in the presence of a hole scavenger.

Both electrons and holes that accumulate within the CdSe nanocrystals contribute to the transient bleaching observed following the band gap excitation. In our early studies[57,58,67] we have demonstrated the factors that dictate the transient bleaching in CdS and CdSe nanoparticles. The initial fast recovery during 2−3 ps can be attributed the Auger processes and charge recombination. Bleaching recovery from trapped charge carriers can occur over a period of several nanoseconds. Excess charges stored on semiconductor particles are known to shift the absorption edge to the blue.[66] In the absence of a hole scavenger the transient bleaching recovers in the submicrosecond time scale. However, depletion of holes from the CdSe surface causes bleaching to sustain over several microseconds. Interestingly, the decay of the oxidation product parallels the bleaching recovery with the appearance of an isosbestic point around 520 nm. Existence of an isosbestic point suggests that the 600 nm transient is the only contributing factor to the transient bleaching. We attribute the capture of excess

electrons by $PPD^{\bullet+}$ and/or reinjection of holes into CdSe as the factors responsible for the long-term recovery of the transient bleaching.

Conclusions

Surface-bound organic molecules play an important role in dictating the excited state dynamics of CdSe nanocrystals. Such surface-bound molecules are known to control on−off emission cycles of the blinking semiconductor quantum dots. The emission and transient absorption measurements presented here compare the behavior of CdSe nanocrystals in the presence of surface modifier (*n*-BA) and a hole scavenger (PPD). Both the emission quenching and formation of the oxidation product in the transient absorption experiments confirm the hole transfer to PPD at the CdSe interface. Most of the fast kinetic spectroscopy studies carried out to date has probed the femtosecond−picosecond processes responsible for bleaching of CdSe nanocrystals. The charge accumulation around the CdSe nanocrystals can extend the lifetime of CdSe bleaching to the submillisecond time scale. For example, formation of PPD cation at CdSe nanocrystal's surface extends the bleaching for hundreds of microseconds. Basic understanding of such interfacial charge transfer processes and charging effects will aid in understanding the blinking behavior of CdSe nanocrystals.

Acknowledgment. The work described herein was supported by the Office of Basic Energy Sciences of the US Department of Energy. This is Contribution No. 4436 from the Notre Dame Radiation Laboratory. We thank Prof. Dan Meisel for helpful discussions.

References and Notes

(1) Peng, X.; Manna, L.; Yang, W.; Wickham, J.; Scher, E.; Kadavanich, A.; Alivisatos, A. P. *Nature* **2000**, *404*, 59.
(2) Gerion, D.; Pinaud, F.; Williams, S. C.; Parak, W. J.; Zanchet, D.; Weiss, S.; Alivisatos, A. P. *J. Phys. Chem. B* **2001**, *105*, 8861.
(3) Collier, C. P.; Vossmeyer, T.; Heath, J. R. *Annu. Rev. Phys. Chem.* **1998**, *49*, 371.
(4) Steigerwald, M. L.; Alivisatos, A. P.; Gibson, J. M.; Harris, T. D.; Kortan, R.; Muller, A. J.; Thayer, A. M.; Duncan, T. M.; Douglass, D. C.; Brus, L. E. *J. Am. Chem. Soc.* **1988**, *110*, 3046.
(5) Steigerwald, M. L.; Brus, L. E. *Acc. Chem. Res.* **1990**, *23*, 183.
(6) Leatherdale, C. A.; Woo, W. K.; Mikulec, F. V.; Bawendi, M. G. *J. Phys. Chem. B* **2002**, *106*, 7619.
(7) Murray, C.; Norris, D.; Bawendi, M. *J. Am. Chem. Soc.* **1993**, *115*, 8706.
(8) Nirmal, M.; Brus, L. *Acc. Chem. Res.* **1999**, *32*, 407.
(9) Krauss, T. D.; O'Brien, S.; Brus, L. E. *J. Phys. Chem. B* **2001**, *105*, 1725.
(10) Koberling, F.; Mews, A.; Basche, T. *Adv. Mater.* **2001**, *13*, 672.
(11) Schlegel, G.; Bohnenberger, J.; Potapova, I.; Mews, A. *Phys. Rev. Lett.* **2002**, *88*, 137401.
(12) Shimizu, K. T.; Woo, W. K.; Fisher, B. R.; Eisler, H. J.; Bawendi, M. G. *Phys. Rev. Lett.* **2002**, *89*, 117401.
(13) Kuno, M.; Fromm, D. P.; Hamann, H. F.; Gallagher, A.; Nesbitt, D. J. *J. Chem. Phys.* **2000**, *112*, 3117.
(14) Ebenstein, Y.; Mokari, T.; Banin, U. *Appl. Phys. Lett.* **2002**, *80*, 4033.
(15) Kuno, M.; Fromm, D. P.; Gallagher, A.; Nesbitt, D. J.; Micic, O. I.; Nozik, A. J. *Nano Lett.* **2001**, *1*, 557.
(16) Wang, L. W. *J. Phys. Chem. B* **2001**, *105*, 2360.
(17) Alfassi, Z.; Bahnemann, D.; Henglein, A. *J. Phys. Chem.* **1982**, *86*, 4656.
(18) Haase, M.; Weller, H.; Henglein, A. *J. Phys. Chem.* **1988**, *92*, 4706.
(19) Krauss, T. D.; Brus, L. E. *Phys. Rev. Lett.* **1999**, *83*, 4840.
(20) Empedocles, S.; Bawendi, M. *Acc. Chem. Res.* **1999**, *32*, 389.
(21) Kumar, A.; Janata, E.; Henglein, A. *J. Phys. Chem.* **1988**, *92*, 2587.
(22) Shim, M.; Shilov, S. V.; Braiman, M. S.; Guyot-Sionnest, P. *J. Phys. Chem. B* **2000**, *104*, 1494.
(23) Seker, F.; Meeker, K.; Kuech, T. F.; Ellis, A. B. *Chem. Rev.* **2000**, *100*, 2505.
(24) Dannhauser, T.; O'Neil, M.; Johansson, K.; Whitten, D.; McLendon, G. *J. Phys. Chem.* **1986**, *90*, 6074.
(25) Kamat, P. V.; de Lind, M.; Hotchandani, S. *Isr. J. Chem.* **1993**, *33*, 47.
(26) Cowdery, C. J. R.; Whitten, D. G.; McLendon, G. L. *Chem. Phys.* **1993**, *176*, 377.
(27) Talapin, D. V.; Rogach, A. L.; Kornowski, A.; Haase, M.; Weller, H. *Nano Lett.* **2001**, *1*, 207.
(28) Chandrasekharan, N.; Kamat, P. V. *Res. Chem. Intermed.* **2002**, *28*, 847.
(29) Landes, C.; Burda, C.; Braun, M.; El-Sayed, M. A. *J. Phys. Chem. B* **2001**, *105*, 2981.
(30) Peng, Z. A.; Peng, X. *J. Am. Chem. Soc.* **2001**, *123*, 183.
(31) Thomas, M. D.; Hug, G. L. *Comput. Chem. (Oxford)* **1998**, *22*, 491.
(32) Alivisatos, P.; Harris, T.; Levinos, N.; Steigerwald, M.; Brus, L. *J. Chem. Phys.* **1988**, *89*, 4001.
(33) Brus, L. *New J. Chem.* **1987**, *11*, 123.
(34) Henglein, A. *Prog. Colloid Polym. Sci.* **1987**, *73*, 1.
(35) Sant, P. A.; Kamat, P. V. *Phys. Chem. Chem. Phys.* **2002**, *4*, 198.
(36) Kortan, A. R.; Hull, R.; Opila, R. L.; Bawendi, M. G.; Steigerwald, M. L.; Carroll, P. J.; Brus, L. E. *J. Am. Chem. Soc.* **1990**, *112*, 1327.
(37) Sasha, G.; Gary, H. *J. Phys. Chem.* **1994**, *98*, 5338.
(38) Rogach, A. L.; Kornowski, A.; Gao, M.; Eychmüller, A.; Weller, H. *J. Phys. Chem. B* **1999**, *103*, 3065.
(39) Henglein, A. *Ber. Bunsen-Ges. Phys. Chem.* **1982**, *86*, 301.
(40) Resch, U.; Weller, H.; Henglein, A. *Langmuir* **1989**, *5*, 1015.
(41) Dabbousi, B. O.; RodriguezViejo, J.; Mikulec, F. V.; Heine, J. R.; Mattoussi, H.; Ober, R.; Jensen, K. F.; Bawendi, M. G. *J. Phys. Chem. B* **1997**, *101*, 9463.
(42) Reiss, P.; Bleuse, J.; Pron, A. *Nano Lett.* **2002**, *2*, 781.
(43) Landes, C. F.; Braun, M.; El-Sayed, M. A. *J. Phys. Chem. B* **2001**, *105*, 10554.
(44) Hu, J.; Li, L.; Yang, W.; Manna, L.; Wang, L.-W.; Alivisatos, A. P. *Science* **2001**, *292*, 2060.
(45) Guyot-Sionnest, P.; Shim, M.; Matranga, C.; Hines, M. *Phys. Rev. B* **1999**, *60*, R2181.
(46) Schmelz, O.; Mews, A.; Basche, T.; Herrmann, A.; Mullen, K. *Langmuir* **2001**, *17*, 2861.
(47) Kamat, P. V.; Dimitrijevic, N. M.; Fessenden, R. W. *J. Phys. Chem.* **1987**, *91*, 396.
(48) Chestnoy, N.; Harris, T. D.; Hull, R.; Brus, L. E. *J. Phys. Chem.* **1986**, *90*, 3393.
(49) Eychmueller, A.; Haesselbarth, A.; Katsikas, L.; Weller, H. *Ber. Bunsen-Ges. Phys. Chem.* **1991**, *95*, 79.
(50) Brus, L. *Isr. J. Chem.* **1993**, *33*, 9.
(51) James, D. R.; Liu, Y.-S.; de Mayo, P.; Ware, W. R. *Chem. Phys. Lett.* **1985**, *120*, 460.
(52) Burda, C.; Link, S.; Mohamed, M.; El-Sayed, M. *J. Phys. Chem. B* **2001**, *105*, 12286.
(53) Klimov, V. I. *J. Phys. Chem. B* **2000**, *104*, 6112.
(54) Zhang, J. Z. *Acc. Chem. Res.* **1997**, *30*, 423.
(55) Zhang, J. Z. *J. Phys. Chem. B* **2000**, *104*, 7239.
(56) Braun, M.; Burda, C.; Mohamed, M.; El-Sayed, M. *Phys. Rev. B* **2001**, *64*, 035317.
(57) Kamat, P. V.; Dimitrijevic, N. M.; Nozik, A. J. *J. Phys. Chem.* **1989**, *93*, 2873.
(58) Kamat, P. V.; Ebbesen, T. W.; Dimitrijevic, N. M.; Nozik, A. J. *Chem. Phys. Lett.* **1989**, *157*, 384.
(59) Henglein, A.; Weller, H. *Photochemical Energy Conversion*; Norris, J. R., Jr., Meisel, D., Eds.; Elsevier: New York, 1989.
(60) Micic, O. I.; Rajh, T.; Comor, M. V. Influence of surface properties on charge carrier dynamics of quantized semiconductor colloids. In *Electrochemistry in Colloids and Dispersions*; Mackay, R. A., Texter, J., Eds.; VCH Publishers: New York, 1992; p 457.
(61) Kamat, P. V. *Chem. Rev.* **1993**, *93*, 267.
(62) Kamat, P. V. Native and surface modified semiconductor nanoclusters. In *Molecular level artificial photosynthetic materials*; Meyer, J., Ed.; Progress in Inorganic Chemistry Series 44; John Wiley & Sons: New York, 1997; p 273.
(63) Tripathi, G. N. R.; Sun, Q. *J. Phys. Chem. A* **1999**, *103*, 9055.
(64) Feng, Y.; Chan, A. *J. Soc. Cosmet. Chem.* **1994**, *45*, 299.
(65) Gutierrez, M.; Henglein, A. *Ber. Bunsen-Ges. Phys. Chem.* **1983**, *87*, 474.
(66) Henglein, A.; Kumar, A.; Janata, E.; Weller, H. *Chem. Phys. Lett.* **1986**, *132*, 133.
(67) Dimitrijevic, N. M.; Kamat, P. V. *J. Phys. Chem.* **1987**, *91*, 2096.